

The Orbital Order Parameter in $\text{La}_{0.95}\text{Sr}_{0.05}\text{MnO}_3$ probed by Electron Spin ResonanceJ. Deisenhofer,¹ B. I. Kochelaev,² E. Shilova,² A. M. Balbashov,³ A. Loidl,¹ and H.-A. Krug von Nidda¹¹Experimentalphysik V, Center for Electronic Correlations and Magnetism,
Institute for Physics, Augsburg University, D-86135 Augsburg, Germany²Kazan State University, 420008 Kazan, Russia³Moscow Power Engineering Institute, 105835 Moscow, Russia

(Dated: April 14, 2024)

The temperature dependence of the electron-spin resonance linewidth in $\text{La}_{0.95}\text{Sr}_{0.05}\text{MnO}_3$ has been determined and analyzed in the paramagnetic regime across the orbital ordering transition. From the temperature dependence and the anisotropy of linewidth and g -value the orbital order can be unambiguously determined via the mixing angle of the wave functions of the e_g -doublet. The linewidth shows a similar evolution with temperature as resonant x-ray scattering results.

PACS numbers: 77.22.Gm, 64.70.Pf

In transition-metal oxides the orbital degrees of freedom play an important role for the electric and magnetic properties. Their coupling to spin, charge and lattice is responsible for the occurrence of a variety of complex electronic ground states. Orbital order (OO) can be derived via the Jahn-Teller (JT) effect or via superexchange (SE) between degenerate orbitals under the control of strong Hund's-rule coupling [1]. Strong correlations exist between spin and orbital order and between OO and lattice distortions, but of course a one-to-one correspondence cannot be expected. While spin and lattice order can easily be detected experimentally, this is not true for OO and so far the OO parameter remains hidden. In recent years resonant x-ray scattering (RXS) has been used to derive information on the OO parameter [2], but there is an ongoing dispute, whether RXS probes the JT distortion or the orbital charge distribution [3, 4]. Indirectly, OO can also be derived from diffraction experiments via lattice distortions and bond lengths [5]. In this Letter we demonstrate that electron-spin resonance (ESR) can be used to detect OO and to monitor the evolution of the OO parameter. Probing the spin of the partially filled d -shell of Mn^{3+} ions by ESR, the anisotropy and T -dependence of g -value and linewidth H provide clear information on OO via spin-orbit (SO) coupling.

The power of ESR to gain insight into OO will be demonstrated on A-type antiferromagnetic (AFM) LaMnO_3 ($T_N = 140$ K), the parent compound of the magnetoresistance manganites and a paradigm for a cooperative JT effect that suggests a $d_{3x^2-r^2}/d_{3y^2-r^2}$ -type OO below $T_N = 750$ K [6]. However, it has been shown that SE interactions play an important role, too [7]. Several recent studies exhibit clear anomalies of the ESR parameters at the JT transition in both doped and pure LaMnO_3 [8, 9, 10, 11]. The orbitally ordered O^0 -phase is characterized by an anisotropy of H [11, 12], which for polycrystalline samples reduces to a broad maximum in $H(T)$ [9, 10]. Previously, the angular dependencies of H and the resonance field H_{res} had been analyzed for 200 K and 300 K in high-temperature approximation, al-

lowing to estimate the Dzyaloshinsky-Moriya (DM) interaction and the strength of the zero-field splitting (ZFS) parameters [13]. At X-band frequencies (9 GHz) H was of the same order of magnitude as H_{res} and due to the overlap with the resonance at H_{res} and their mutual coupling via the nondiagonal elements of the dynamic susceptibility [14] the values for H_{res} contained a rather large uncertainty. To avoid these problems we performed new experiments at Q-band frequencies (34 GHz), which allowed a better determination of H_{res} .

The scope of the present paper is the comprehensive analysis of the T -dependence and anisotropy of H and the g -value of the ESR signal in $\text{La}_{0.95}\text{Sr}_{0.05}\text{MnO}_3$. We chose this concentration for the present study as an untwinned single crystal was available and $T_{\text{JT}} = 605$ K is accessible to our experimental setup [15].

New ESR measurements were performed with a Bruker ELEXSYS E500 CW spectrometer at Q-band frequencies (34 GHz, 4.2 K $T = 290$ K), using a continuous gas-flow cryostat for He (Oxford). The oriented sample was mounted in a quartz tube with para. A goniometer allowed the rotation of the sample around an axis perpendicular to the static magnetic field H_{ext} .

Figure 1 shows H for X-band frequency and Fig. 2 H and the effective g -value $g_e = h/(g_{\text{B}} H_{\text{res}})$ determined from H_{res} for Q-band frequency. The observed linewidths at both frequencies nicely coincide. Only near them inimum below 200 K the absolute values are slightly enhanced at 34 GHz as compared to 9 GHz. Whereas the g -values obtained at X-band frequency bear a rather large uncertainty [11, 13], at Q-band frequency the g -values show a regular T -dependence, approaching a constant high-temperature value and increasing for $T \rightarrow T_N$. First, we determined the ZFS parameters D and E from the T dependence of H_{res} at Q-band frequency. Using the general formula for the resonance shift due to crystal field (CF) effects [13, 16] and accounting only for the rotation (angle θ) of the MnO_6 octahedra in the ac plane (axis notation like in Ref. 17), we obtained the following expressions for the effective g -values for H_{ext} applied

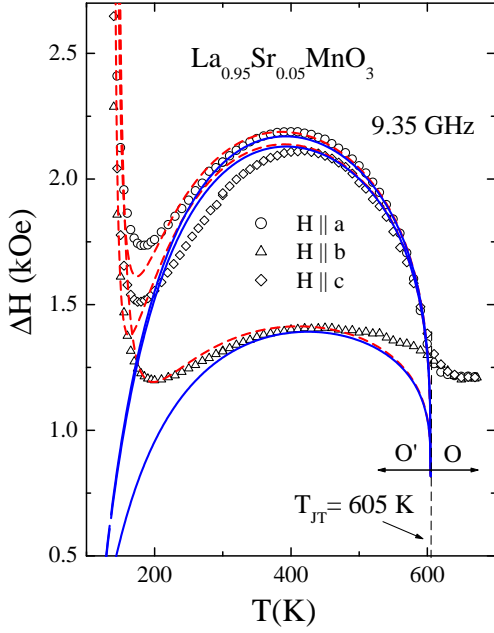


FIG. 1: $\Delta H(T)$ in $\text{La}_{0.95}\text{Sr}_{0.05}\text{MnO}_3$ at X-Band frequency for H_{ext} applied parallel to the three main axes of the orthorhombic structure. Solid and dashed lines represent fits using eq. (2) as described in the text.

along one of the crystallographic axes

$$\frac{g_{a,c}^e(T)}{g_{a,c}^e} = 1 + \frac{D}{T - T_{CW}} [(3 \cos^2 \theta - 1) - 3(1 + \cos^2 \theta) \sin^2 \theta] \quad (1)$$

$$\frac{g_b^e(T)}{g_b^e} = 1 - \frac{2D}{T - T_{CW}} (3 \cos^2 \theta - 1);$$

with the Curie-Weiss (CW) temperature T_{CW} and $D = E = D$. All terms of second and higher order in $D = (T - T_{CW})$ were neglected. The T -dependence of the effective g -values is, hence, given by the CW law of the magnetic susceptibility. Excluding the critical regime on approaching magnetic order below 170 K, the data are well described by this approach (solid lines in Fig. 2), where T_{CW} was kept fixed at 111 K [11]. The rotation angle was chosen as $\theta = 13^\circ$ as observed in pure LaMnO_3 [5, 17]. Then all data can be consistently described by $D = 0.60(2)$ K, the $E = D$ ratio $= 0.37(1)$, and the g -values $g_a = 1.988(1)$, $g_b = 1.986(1)$, and $g_c = 1.984(1)$. From these crystallographic g -values, the local g values of Mn^{3+} can be calculated as $g_z = 1.977$, $g_y (= g_b) = 1.986$, and $g_x = 1.995$, typical for ions with less than half-filled 3d-shell with the longest and shortest Mn-O bond along the local z and x direction, respectively [18].

The main result of this evaluation is the $E = D$ ratio, which we improved in comparison to our previous estimate [13] by the Q-band experiment. For H_{ext} applied along the b -axis the data are nearly T -independent, whereas they clearly exhibit the CW behavior for the other orientations. Regarding the equation for g_b , this is

only possible, if the factor $(3 \cos^2 \theta - 1)$ is close to zero and hence $\theta = 45^\circ$. This result is independent on the value of the rotation angle θ . Only the absolute value of D directly depends on the choice of θ , which accounts for the splitting of the resonance fields between a and c direction.

With the obtained $E = D$ ratio we now turn to the evaluation of the linewidth data. A detailed derivation of the CF contributions to the ESR linewidth in the cooperative JT distorted perovskite structure accounting for the mutual rotations of the MnO_6 octahedra is presented in Ref. 19. These theoretical considerations can be summarized in the following formula

$$\Delta H^{(\#; \#')}(T) = \frac{T - T_{CW}}{T} [f_{DM}(1) + f_{CF}(1) f_{reg}^{(\#; \#')}] + \frac{1}{T_{JT}} \left[\frac{T}{T_{JT}} \right]^2 (f_{CF}(1) f_{reg}^{(\#; \#')}) + f_{CFD} \frac{T_N}{6(T - T_N)} f_{div}^{(\#; \#')}]; \quad (2)$$

where the first term describes the contribution $f_{DM}(1)$ of the DM interaction as introduced by Huber et al. [8] assuming that the exchange constants are T -independent. This contribution is expected to survive the JT transition and hence to determine the line broadening also at $T > T_{JT}$. The second and third term, f_{CF} and f_{CFD} , represent the regular and divergent CF contributions, respectively. Only the latter diverges for $T \rightarrow T_N$ with an exponent β , whereas both terms decrease for $T \rightarrow T_{JT}$ with a critical exponent $2 - \beta$, with β being the critical exponent of the ZFS parameters D and E . Note that both the assumption of T independent exchange constants and the application of the criticality at T_{JT} throughout the entire paramagnetic O^0 -phase can influence the value of the critical exponent which therefore has to be regarded cautiously. The angular factors $f_{reg}^{(\#; \#')}$ and $f_{div}^{(\#; \#')}$ read

$$f_{reg}^{(\#; \#')} = f_{div} + (1 + \cos^2 \theta) (1 + \frac{3}{2} \sin^2 \theta);$$

$$f_{div}^{(\#; \#')} = \frac{1}{2} [1 - 3 \cos^2 \theta + 2(1 + \cos^2 \theta)^2 (1 - \sin^2 \theta \sin^2 \theta')] + \frac{1}{2} [1 - 3 \cos^2 \theta - 2(1 + \cos^2 \theta)^2 (1 - \sin^2 \theta \cos^2 \theta')];$$

where θ and θ' are the polar and azimuthal angles between H_{ext} and the crystallographic b and c axes, respectively. An analogous calculation to the one presented in [19] showed that the DM interaction does not exhibit any critical behavior at T_N . To minimize the number of fit parameters, we neglected here any angular dependence of the DM contribution. In first approximation this is justified by the observation that above T_{JT} the linewidth is isotropic. However, generally an anisotropy of the DM contribution can arise in the orbitally ordered state [13]. But it consists itself at least in two contributions from different Mn-O-Mn bond geometries, and

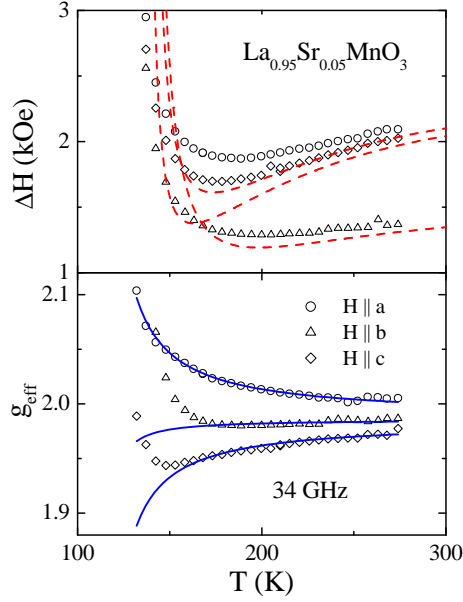


FIG. 2: $\Delta H(T)$ and effective g -value $g_e(T)$ at Q-band frequency for H_{ext} applied parallel to the three crystallographic axes of the orthorhombic structure. The solid lines represent fits using eq. (1) for g_e , the dashed lines for ΔH are the same as in Fig. 1.

its transformation to an isotropic behavior on approaching T_{JT} needs further theoretical considerations. In the minimum model we omitted the divergent CF contribution ($C_{FD} = 0$) and tried to find the best fit for the linewidth data. The characteristic temperatures were kept fixed at $T_{CW} = 111$ K and $T_{JT} = 605$ K and the rotation angle in the ac plane was set to $\phi = 13^\circ$. In addition the parameter $\alpha = 0.37$ was taken from the evaluation of the g -values. So only three fit parameters remain, as there are the regular part of the CF contribution $C_{CF}(1)$, its critical exponent at the JT transition, and the DM contribution $D_{DM}(1)$, which survives also at temperatures $T > T_{JT}$. A simultaneous fit (solid lines in Fig. 1) of the T -dependence of ΔH is satisfactorily performed above 200 K with $D_{DM}(1) = 1.0(1)$ kOe, $C_{CF}(1) = 0.57(2)$ kOe, and $\alpha = 0.16(1)$.

Finally, we added the effect of the divergent CF contribution, which allows to increase the difference between H_a and H_c to lower temperatures, as observed in the experiment. As shown in Fig. 1 (dashed lines) a satisfactory qualitative description of the data was obtained by $C_{FD} = 10$ kOe and $\alpha = 1.8$ with fixed $T_N = 135$ K. Comparison with the Q-band data Fig. 2 indicates that the magnetic critical exponent below 200 K rather turns to the theoretically expected lower value of $\alpha = 0.75$ [19], which however is not applicable at higher temperatures. The reason is that the fit function is used for the whole temperature range, but the derivation of the power law only holds for temperatures close to T_N . A further improvement may be achieved by taking into account the sym-

metric anisotropic exchange interaction, which is beyond the scope of this paper. In the following we concentrate on the information obtained from the regular part of H .

The DM contribution $D_{DM}(1) = 1.0$ kOe determined in the O^0 -phase is lower than the one expected from $H = 1.4$ kOe in the O -phase. This discrepancy can be explained by linewidth contributions of the CF due to the dynamic JT effect present in the O -phase [20]. Comparison with the regular CF contribution $C_{CF}(1) = 0.57$ kOe allows to estimate the averaged value D_{DM} of the DM interaction as defined in Ref. 8. The ratio of the linewidth contributions equals the ratio of the respective second moments approximated by $10(D_{DM} = D)^2$ $D_{DM}(1) = C_{CF}(1)$ [8]. With $D = 0.6$ K one obtains $D_{DM} = 0.25$ K. These values are free from the uncertainty in the estimation of the exchange frequency in the exchange-narrowed linewidth [19], because we used the g -values to determine the absolute values. They are smaller than the values estimated earlier for polycrystalline LaMnO₃ but their relative strength is in good agreement with previous results [8, 9].

After having extracted the ZFS parameters we will now discuss the consequences for OO in LaMnO₃: In Fig. 3(a) the reduced ESR linewidth $H_a(T) = (T/T_{CW})$ for H_{ext} parallel to the a -axis, which bears the critical behavior on approaching T_{JT} (see eq. 2), and the RXS intensity obtained by Murakami et al. [2] for LaMnO₃ are shown to visualize the similarity of the two quantities on approaching both T_N and T_{JT} . Note that we used the fixed value $T_{CW} = 111$ K of the O^0 -phase leading to somewhat lower values for the O -phase. It has been pointed out that the RXS intensity close to T_{JT} is $\propto (1 - T/T_{JT})^2$ [4], where α denotes the critical exponent of the OO parameter given by the pseudo spin $T = 1/2(\sin \phi; 0; \cos \phi)$ [4, 23]. The angle $\phi = 2\arctan(c_2/c_1)$ is a measure of the mixing of the wave functions of the e_g -doublet in the ground state $\psi_g = c_1\beta z^2 - r^2 + c_2\beta x^2 - y^2$. To compare the results of RXS and ESR we fitted the RXS data in the vicinity of the JT transition (650 K $< T < T_{JT} = 780$ K) with such a critical behavior (solid line in Fig. 3(a)) and obtained an exponent $\alpha = 0.16(1)$ in agreement with the ESR linewidth. Considering that the ZFS parameters can be denoted as $D = 3(\alpha + \beta^2) \cos \phi$ and $E = \frac{1}{3}(\alpha + \beta^2) \sin \phi$ with the spin-spin coupling β , the SO coupling and the t_{2g} - e_g splitting energy [18], it is easy to identify the relation with the OO parameter T . Despite the lack of data in the critical regime, Fig. 3(b) shows the orbital mixing coefficients c_1 and c_2 determined from a neutron diffraction (ND) study by Rodríguez-Carjaval et al. [5] The dashed lines were obtained by using $K(1 - T/T_{JT})^{\alpha} + 2^{-1/2}$ ($T_{JT} = 750$ K) with a critical exponent $\alpha = 2$ provided by $D/(c_1^2 - c_2^2)$ and $E/c_1 - \beta$. With $K_1 = 0.10$ and $K_2 = -0.12$ the data for c_1 and c_2 can be well described throughout the JT distorted phase. However, attempting to describe the three

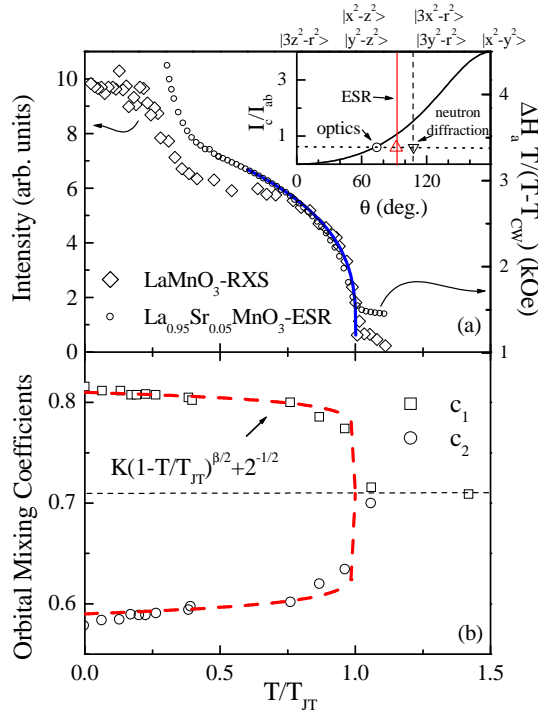


FIG. 3: T-dependence of (a) the reduced ESR linewidth in $\text{La}_{0.95}\text{Sr}_{0.05}\text{MnO}_3$ compared to the RXS intensity of LaMnO_3 taken from [2]. The solid line is a fit of the RXS intensity as described in the text. Inset: T-dependence of the normalized optical spectral weight $I_c = I_{ab}$ following [21] (solid line) with the experimentally derived values; (b) T-dependence of c_1 and c_2 determined by ND taken from [5]. The dashed lines were obtained using $K(1 - T/T_{JT})^{3/2} + 2^{-1/2}$.

data points in the critical regime rather suggest ≈ 0.3 . Only a detailed structural study in the critical regime will allow a direct confirmation of the critical exponent for c_1 and c_2 , but $\approx 2 = 0.08$ seems to yield a reasonable description.

The main result of this study is to estimate the angle $\approx 3 \arctan(E/D)$ and determine the type of OO by using the obtained value $E/D = 0.37(1)$, which after taking into account the transformation to a local coordinate system [19] results in $\approx 92^\circ$. Another estimate has been obtained from ND via the orbital mixing coefficients at room temperature $c_1 \approx 0.8$ and $c_2 \approx 0.6$ resulting in $\approx 106^\circ$ [5]. This discrepancy cannot easily be explained. However, Tobe et al. tried to explain the anisotropy of the optical conductivity in LaMnO_3 on the basis of a $p-d$ transition model by using the ratio $I_c = I_{ab} = 2(1 - \cos \theta) = (2 + \cos \theta)$ (see inset of Fig. 3(a)) between the optical spectral weight with the polarization within the ferromagnetic (FM) plane (there ab) and along the AFM axis (there c). [21] Their simple model suggests a value $\approx 74^\circ$ to describe the experimental value of $I_c = I_{ab} = 0.6$ at 10 K in the AFM regime. Theoretically, only a slight decrease of θ below T_N is expected

[7, 22] and therefore above T_N $\approx 92^\circ$ yields a better description of the anisotropic properties of LaMnO_3 in the orbitally ordered state than $\approx 106^\circ$. Alejandro et al. derived a similar E/D -value from ESR data in $\text{La}_{0.78}\text{Sr}_{0.22}\text{MnO}_3$ [12] which confirms our result. To the best of our knowledge no estimate has been obtained by RXS and it is worthwhile to note that the RXS intensity becomes maximal for $\theta = 90^\circ$ [4], the value obtained by ESR. Following [23] $\theta = 90^\circ$ characterizes OO stabilized by the SE processes in the FM bonds and the electron-phonon coupling is small compared to the bandwidth. Recent calculations suggest $\theta = 90^\circ$ at $T = T_N$ and $\approx 83^\circ$ at $T = 0$ and confirm our findings [22].

In summary, we were able to determine unambiguously the orbital order of $\text{La}_{0.95}\text{Sr}_{0.05}\text{MnO}_3$. The evolution of the OO parameter monitored by the RXS intensity shows an intriguing similarity to the ESR linewidth. We found a mixing angle $\approx 92^\circ$ suggesting that OO is dominated by SE coupling in agreement with theoretical predictions.

We thank M.V. Eremkin, T. Kopp, and K.-H. Hock for fruitful discussions. This work was supported by the BMFT under contract No. 13N 6917 (EKM) and partly by the DFG via the SFB 484 and DFG/RFFI-project No. 436-RUS 113/566/0. B.J.K. and E.S. were partially supported by CRDF via grant REC-007.

-
- [1] H.A. Jahn and E. Teller, Proc. R. Soc. London 161, 220 (1937); K.I. Kugel and D.I. Khomskii, Sov. Phys. Usp. 25, 231 (1982).
 - [2] Y. Murakami et al., Phys. Rev. Lett. 81, 582 (1998).
 - [3] P. Benedetti et al., Phys. Rev. B 63, 060408 (2001).
 - [4] S. Ishihara et al., Rep. Prog. Phys. 65, 561 (2002).
 - [5] J. Rodriguez-Carvajal et al., Phys. Rev. B 57, R3189 (1998).
 - [6] J.B. Goodenough, Phys. Rev. 100, 564 (1955).
 - [7] S. Okamoto et al., Phys. Rev. B 65, 144403 (2002).
 - [8] D.L. Huber et al., Phys. Rev. B 60, 12155 (1999).
 - [9] M. Tovar et al., Phys. Rev. B 60, 10199 (1999).
 - [10] J. Deisenhofer et al., Phys. Rev. B 66, 054414 (2002).
 - [11] V.A. Ivashin et al., Phys. Rev. B 61, 6213 (2000).
 - [12] G. Alejandro et al., Physica B 320, 26 (2002); private communication.
 - [13] J. Deisenhofer et al., Phys. Rev. B 65, 104440 (2002).
 - [14] H. Benner et al., J. Phys. C 16, 6011 (1983).
 - [15] M. Paraskevopoulos et al., J. Phys.: Condens. Matter 12, 3993 (2000); A. Pimenov et al., Phys. Rev. B 62, 5685 (2000).
 - [16] N.O. Moreno et al., Phys. Rev. B 63, 174413 (2001).
 - [17] Q. Huang et al., Phys. Rev. B 55, 14987 (1997).
 - [18] A. Abragam and B. Bleaney, Electron Paramagnetic Resonance of Transition Ions, (Clarendon, Oxford, 1970).
 - [19] B.I. Kochelaev et al., to be published.
 - [20] M.C. Sanchez et al., Phys. Rev. Lett. 90, 045503 (2003).
 - [21] K. Tobe et al., Phys. Rev. B 64, 184421 (2001).
 - [22] O. Sikora et al., Acta Phys. Pol. B 34, 861 (2003).
 - [23] R. Marezono et al., Phys. Rev. B 58, 11583 (1998).